Drug-Controlled anti-PD-1 CAR T Cells to Target the Replication-Competent Reservoir in T_{FH} Cells.

Karsten Eichholz[1], Yoshinori Fukazawa[2], Christopher W. Peterson[1], Francoise Haeseleer[1], Manuel Medina[2], Shelby Hoffmeister[2], Derick Duell[2], Benjamin Varco- Merth[2], Sandra Dross[3], Haesun Park[2], Caralyn Labriola[2], Michael Axthelm[2], Robert Murane[4], Jeremy Smedley[2], Lei Jin[1], Jiaxin Gong[1], Rust Blake[1], Deborah Fuller[5], Hans-Peter Kiem[1], Louis J. Picker[2], Afam Okoye[2], Larry Corey[1,6]

[1]Fred Hutchinson Cancer Center, Seattle, WA,[2]Vaccine and Gene Therapy Institute, Beaverton, OR and Oregon Health & Science University, Beaverton, OR, [3]Department of Microbiology, Seattle, WA,[4]Washington National Primate Research Center, Seattle, WA,[5]Department of Microbiology, Seattle, WA

[6]Department of Medicine and Laboratory Medicine, Seattle, WA,

Abstract

Background: Programmed cell death protein 1 (PD-1) is an immune checkpoint marker expressed on memory T cells and enriched in latently-infected CD4+ T cells and T follicular helper cells (T_{FH}) containing replication-competent human immune deficiency virus 1 (HIV) provirus in people with HIV on antiretroviral therapy (ART).

Methods: We recently tested a novel anti-PD-1 chimeric antigen receptor (CAR) T cell approach *in vivo* in simian immunodeficiency virus (SIV) mac239-infected and SIV-naïve rhesus macaques (RMs) to assess the impact of PD-1 depletion on viral reservoirs and rebound dynamics.

Results: We found that anti-PD-1 CAR T cells expanded efficiently and rapidly eradicated all T_{FH} cells from the germinal centers with concomitant depletion of detectable SIV RNA from this sanctuary site. This occurred even before release from ART. The anti PD-1 Car T cells persisted for up to 100 days concomitant with the depletion of PD-1+ memory T cells in blood and tissues, resulting in off target immune depletion and a marked increase in SIV replication in extrafollicular portions of lymph nodes, a 2-log higher plasma viremia relative to controls and accelerated disease progression, associated with the acute depletion of CD8+ memory T cells after CAR T expansion. The rapid depletion of T_{FH} sanctuary site in GC while on ART offered the potential to an important advance in the quest for HIV cure if we could develop a second-generation product that had less off target long term effects.

Towards these ends, we integrated a Hepatitis C virus-derived non-structural protein 3 (NS3)-based ON switch into the intracellular domain of our anti-PD-1 CAR (NS3) T cell platform that can be controlled exogenously by administration of a NS3-specific protease inhibitor Grazoprevir (GZV). Mechanistically, the NS3 domain undergoes autocleavage in absence of GZV, thus abrogating any CAR signaling and CAR T cell function. In vitro, primary T cells expressing the anti-PD-1 CAR NS3 kill PD-1+ cells and secret IFNγ in presence of GZV in a dose-dependent manner indicating that the NS3 domain functions as an ON switch.

Conclusions: Combined, these data indicate that a drug-controlled anti-PD-1 CAR NS3 is highly functional and can be controlled exogenously through administration or withdrawal of GZV. These data warrant further investigation of drug controlled-anti-PD-1 CAR T cells in ART-treated SIVmac239-infected rhesus macaques to transiently deplete T_{FH} cells to determine their contribution to the latent reservoir.

Development of the anti-PD-1 CAR

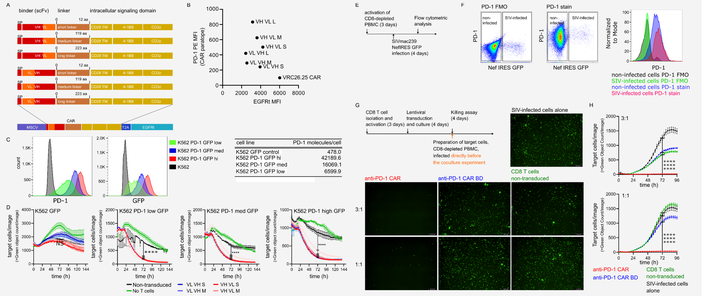


Figure 1: Anti-PD-1 CAR T cell kill PD-1+ cells and inhibit viral replication in vitro. Six anti-PD-1 CARs, which differ in the VH VL orientation of the pembrolizumab-derived scFv and the linker length (S, M and L) between the transmembrane domain and scFv and were cloned in a SIV-based lentiviral vector under the control of a MSCV promoter. The CAR expression cassette contains also a truncated EGFRt for marking downstream of the CAR with a t2a self-cleaving peptide. CAR and EGFRt are interspersed with a t2a self-cleaving peptide (A). The six anti-PD-1 CAR constructs vary in their paratope accessibility assessed with a PD-1 Fc probe (B). Generation of PD-1-GFP+ K562 target cells (C). Curves of a live cell microscopy killing assay of primary anti-PD-1 CAR CD8+ T cells with K562 PD1-GFP with low, medium and high PD-1 expression or K562 GFP control cells (D). Experimental scheme of in vitro SIVmac239 NefIRESGFP-infection (E) to assess PD-1 expression on SIV-infected RM CD4+ T cells (F). Experimental scheme of a killing assay with CAR T cells and target cells infected with SIVmac239 NefIRESGFP (G). Representative images of GFP+ SIV-infected CD4+ T cells at the end of the 96 h coculture with effector cells (anti-PD-1 CAR, binding-deficient PD-1 CAR BD and non-transduced CD8+ T cells) at the indicated E:T ratio (G). Quantification of GFP+ cells in the images acquired over 96 h in the killing assay described in G (H). Shown is one representative experiment out of three. Average cytotoxicity ± SEM of one representative experiment is shown. Statistics were analyzed using a 2-way ANOVA with Tukey's multiple comparisons test at each time point. Results for 72 h are reported. **** = p<0.0001.

Conclusion: Anti-PD-1 CAR T cells are highly efficient in killing PD-1+ cells and prevent viral replication in vitro

Anti-PD-1 CAR T cells deplete T_{FH} cells and prevent viral replication in germinal centers in ART-treated SIV-infected rhesus macaques; associated depletion of PD-1+ CD8 T cells increases viral replication in extrafollicular areas

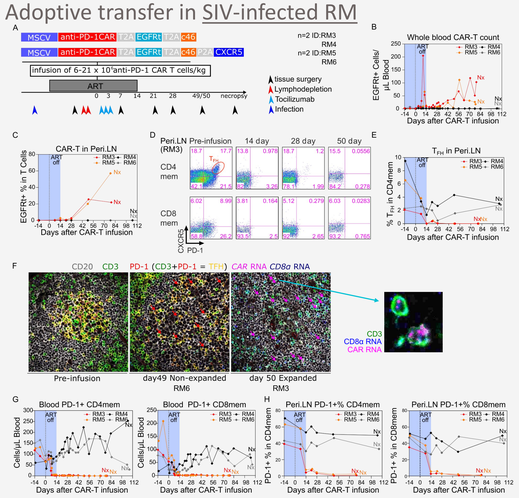


Figure 2: Anti-PD-1 CAR T cells deplete PD-1+ T cells in SIV-infected RM on ART. Schematic of the in vivo animal study (n=4). Dates for tissues surgery, lymphodepletion, duration of ART and tocilizumab treatment are noted (A). Absolute count of EGFRt-expressing CD3+ T cells in peripheral blood for the duration of the study (B). Longitudinal EGFRt-expressing CD3+ T cells in peripheral lymph nodes (Peri.LN) (C). Flow cytometric analysis of PD-1 and CXCR5 expression on CD4+ and CD8+ total memory T cells in Peri.LN from RM3 (D). Frequency of follicular helper T cells (T_{FH}) in CD4+ total memory T cells (E). Combined immunofluorescence and RNA FISH staining on lymph node tissue section for CD20 (grey), CD3 (green), PD-1 (red), CD8α RNA (blue) and CAR RNA (magenta) (F). Magenta arrows point to intrafollicular CD8+ CAR T cells, red arrows point to residual T_{FH} cells post-infusion. T_{FH} cells are characterized by CD3 and PD-1 dual staining within the B cell follicle and appear yellow (F). Absolute count of PD-1+ CD4+ and CD8+ memory T cells in peripheral blood (G). PD-1 expression on Peri.LN CD4+ memory T cells and CD8+ memory T cells (H).

Similar observations were made in SIV-naïve RM

Conclusion: Anti-PD-1 CAR T cells expanded in 3 out of 6 RM. Anti-PD-1 CAR T cells deplete PD-1+ CD4+ and CD8+ T cells as well as T_{FH} cells and enter germinal centers in SIV-naïve and SIV-infected RMs

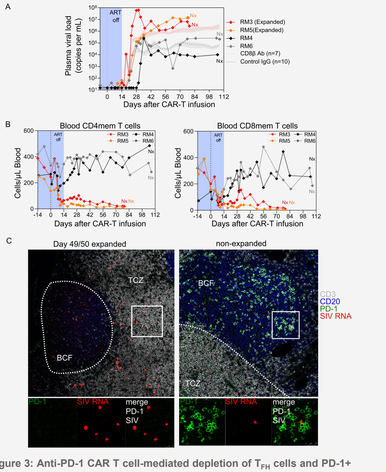


Figure 3: Anti-PD-1 CAR T cell-mediated depletion of T_{FH} cells and PD-1+ T cells do not prevent viral recrudescence after removal of ART. Plasma viral load in the four animals during the anti-PD-1 CAR T cell treatment and after removal of ART. For comparison, historical controls from CD8 T cell-depletion study are added (A). Absolute count of CD4+ memory and CD8+ memory T cells in blood (B). Combined immunofluorescence and RNA FISH staining on lymph node tissue section for CD3 (grey), CD20 (blue), PD-1 (green), SIV RNA (red) ~50 days post-infusion on lymph node sections from RMs with or without CAR T cells expansion(C).

Conclusion: Anti-PD-1 CAR T cells prevent viral replication in the GC; higher viral rebound and extrafollicular replication in RM with CAR T cell expansion is associated with loss of memory CD8 and development of immunodeficiency.

Controlling CAR T cell activity: Integration of a drug-controlled NS3 protease ON switch into the anti-PD-1 CAR signaling domain

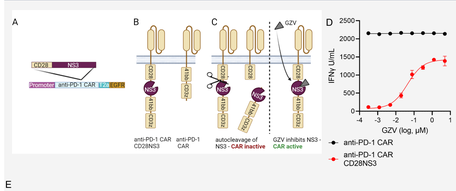
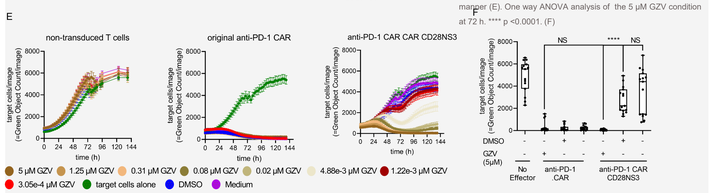


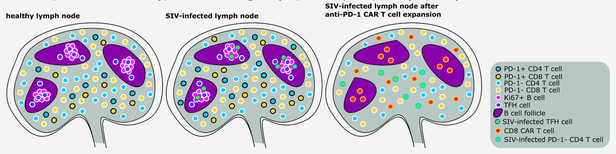
Figure 4: Integration of Hepatitis C virus nonstructural protein 3 (NS3) derived protease into the CAR signaling domain allows exogenous control of CAR function through a small molecule inhibitor. A CD28 NS3 domain (*Li et al., 2022 Cancer Cell, 40, 1294-1305*) (A) was added to the CAR signaling domain between the TM and CAR 41bb CD3ζ (ICD) domain (B). This leads to autocleavage of the ICD and CAR inactivation (C). Addition of a NS3 inhibitor (e.g. Grazoprevir (GZV) permits CAR signaling as ICD sasy connected with the CAR polypeptide (C). The novel anti-PD-1 CAR CD28 NS3 secretes IFNγ in presence of (D) and kills PD-1+ GFP+ target cells in GZV-dose depended manner (E). One way ANOVA analysis of the 5 µM GZV condition at 72 h. **** p <0.0001. (F)



Conclusion: The integration of the NS3 protease domain allows exogenous control of the anti-PD-1 CAR and will be used to study temporary depletion of PD-1+ cells in vivo .

Key Findings, Conclusion and Outlook

- **Anti-PD-1 CAR T cells expand in non-infected and SIV-infected rhesus macaques.**
- Anti-PD-1 CAR CD8+ T cells infiltrate B cell follicles.
- **Anti-PD-1 CAR T cells deplete T_{FH} cells and PD-1+ memory T cells in lymph nodes.**
- **Depletion of Germinal Center T_{FH} cells prevented viral replication in the B cell follicles.**
- **Depletion of memory CD8+ T cells shifted viral replication to the T cell zone and is likely the cause for the higher plasma viral load in animals with CAR T cell expansion.**
- Loss of Ki67+ GC B cells was observed, potentially due to loss of T_{FH} cells.
- Development of LCV+ atypical non-Hodgkin lymphoma (NHL)-like lymphocytosis



- Anti-PD-1 CAR T cells show great promise to target a key cell population involved in HIV persistence.
- Additional safety features need to be implemented in our CAR T cell approach to make it clinically useful.
- **Integration of the NS3 domain into the anti-PD-1 CAR permits exogenous CAR T cell control through GZV administration and will be used to study the effects of temporary depletion of PD-1+ T cells in SIV-infected ART-treated RM.**

Acknowledgements: This independent research was supported by National Institute of Health grant UM1 A126623 and by the Gilead Sciences HIV Cure Grant Program. This research was supported by the Experimental Histopathology Shared Resource and the Cellular Imaging Shared Resource (CISR) of the Fred Hutch/University of Washington Cancer Consortium (P30 CA015704).

This research was supported by the vector production core which is part of Cooperative Centers of Excellence in Hematology NIDDK Grant U54 DK106829. This research was supported by the Integrated Pathology Core at the Oregon National Primate Research Center by NIH Award S10RR024585. The content is solely the responsibility of the authors and does not necessarily represent the official views of the National Institutes of Health.

Primate work at the Washington National Primate Research Center and Oregon National Primate Research Center were supported by U42 (U42OD011123 and U42OD010426) and P51 (P51OD010425 and P51OD011092) grants through the NIH Office of Research Infrastructure Programs (ORIP)

Viral load analyses were performed by the Quantitative Molecular Diagnostics Core of the AIDS and Cancer Virus Program of the Frederick National Laboratory supported in part with Federal Funds from the National Cancer Institute, National Institutes of Health, under contract(s) HHSN261200800001E and 75N91019D00024. The content of this publication does not necessarily reflect the views or policies of the Department of Health and Human Services, nor does mention of trade names, commercial products, or organizations imply endorsement by the US Government.